The method is described as follows. A flow of air emerging from a convergent nozzle (Fig. 2a) can be divided into two regions: a large region of inviscid flow represented by the central streamline AA′ and a thin viscous region near the wall represented by streamline BB′. A fluid particle which moves from A to A′ undergoes isentropic changes, while a particle traveling along BB′ undergoes nonisentropic changes. If the reservoir temperature is uniform, i.e., $T_A = T_B$, then the temperature at B′ is higher than that at A′ and the density at B′ is lower than that at A′. The temperature at A′, $T_{A'}$, can be determined using the isentropic relation

$$T_{A'} = T_0 [1 + (\gamma - 1)/2 \cdot M_e^2]^{-1} \quad (1)$$

where T_0 is the reservoir temperature, M_e the jet exit Mach number, and γ the specific heat ratio. Since M_e is greater than zero, $T_{A'}$ is always less than T_0. In most aerodynamic experiments, the reservoir temperature is kept the same as the ambient temperature (T_a), i.e., $T_0 = T_a$. Therefore, $T_{A'}$ is less than T_a. As a result, the density at A′, $\rho_{A'}$, is greater than the ambient density ρ_a because the static pressure at the jet exit is equal to the ambient pressure. The variations of density and density gradient across the jet exit are sketched in Fig. 2b. The density gradient profile represents the contrast in the schlieren picture (Fig. 1a). The present method is to adjust T_0 according to Eq. (1) so that $T_{A'}$ is equal to T_a and then $\rho_{A'}$ is also equal to ρ_a. However, the temperature at B' is still higher than $T_{A'}$ and the density at B′ is lower than $\rho_{A'}$. The resulting density and its gradient across the jet exit are sketched in Fig. 2c. Comparing the two density gradient profiles (Figs. 2b and 2c), it is seen that the present method (Fig. 2c) produces a larger variation of density gradient in the shear layer, which results in a sharper image. It is noted that the density gradient shown in Fig. 2c is similar to the second derivative of the density profile in Fig. 2b, which gives the greater visual appeal of the shadow effect. However, the schlieren method is known to be superior to the shadowgraph due to its higher sensitivity and better focusing ability. Therefore, the enhancement obtained with the method described is that it makes use of the best features of both the shadow and schlieren methods.

This method has been used successfully to obtain schlieren photographs of the jet at exit Mach numbers of 0.1-0.5 (see Fig. 3). The particular reservoir temperatures required for these conditions are 0.6-15°C above ambient. The corresponding density changes are less than 5% of the reservoir air density. Due to the small changes in temperature and density required by the method, it is expected that no significant effects of heating on flow properties, such as the jet velocity distribution, spreading rate, and heating of the ambient air, would be encountered.

Acknowledgment

This work was supported by the Air Force Office of Scientific Research, Contract F49620-79-0189.

References

[1] Moore, C. J., "The Role of Shear-Layer Instability Waves in Jet Exhaust Noise," *Journal of Fluid Mechanics*, Vol. 80, Pt. 2, 1977, pp. 321-367.

[2] Crow, S. C. and Champagne, F. H., "Orderly Structure in Jet Turbulence," *Journal of Fluid Mechanics*, Vol. 48, Pt. 3, 1971, pp. 547-591.

[3] Hsia, Y., Krothapalli, A., Baganoff, D., and Karamcheti, K., "The Structure of a Subsonic Compressible Rectangular Jet," Joint Institute for Aeronautics and Acoustics, Stanford University, Stanford, Calif., Rept. TR-43, Jan. 1982.

Ignition in Gun Exhaust Plumes

E. M. Schmidt*
Ballistic Research Laboratory, USAARRADCOM
Aberdeen Proving Ground, Maryland

Introduction

SECONDARY combustion is an undesirable signature of both gun and rocket plumes. While the latter are generally steady exhausts from two-dimensional, supersonic nozzles with moderate underexpansion, gun plumes[1] are transient and issue sonically at high pressure from the weapon muzzle. In addition, cannon frequently employ three-dimensional nozzles, called muzzle brakes, to reduce recoil. This Note examines the influence of both transient and three-dimensional flow on the probability of ignition in gun plumes.

Potential sources of ignition include viscous heating in lateral shear layers, hot particles, burning propellant grains, or tracers in the base of the projectile; however, experiments by Carfagno[2] point out the importance of the propellant gas recompression through the large Mach disks typical of gun plumes. Based upon his results, Carfagno proposes a model that assumes a one-dimensional expansion through a normal shock to ambient pressure followed by steady mixing with the surrounding air. The properties of the propellant gas/air mixture are assumed to be a uniform function of the mass of air entrained in the plume, permitting the mixture temperature to be defined as

$$\bar{T} = [rC_{p_\infty} T_{s_\infty} + (1-r) C_{p_1} T_{s_1} - (1-r)^2 u_1^2/2] / [rC_{p_\infty} + (1-r) C_{p_1}] \quad (1)$$

$$r = m_\infty / (m_\infty + m_1) \quad (2)$$

Carfagno makes no attempt to evaluate the details of the mixing process, but assumes that all values of r between zero and one are permissible. Ignition occurs when the local mixture temperature, $\bar{T}$, exceeds certain limits. The limits are established in shock tube experiments using various combinations of air and combustion products as test gases. The ignition temperature limits are relatively insensitive to propellant composition and mixture ratio for $0.2 < r < 0.8$; however, significant changes are associated with the addition of relatively small amounts of flash suppressants, such as potassium sulfate or nitrate (Fig. 1).

Yousefian[3] uses finite difference computations to analyze the mixing and chemistry in the gun plume downstream of the Mach disk. To obtain initial conditions, empirical correlations define the inviscid shock structure of the plume. The axial location of the Mach disk is that given by

$$X/D = 0.69(\gamma p^*/p_\infty)^{1/2} \quad (3)$$

Using a relation derived from core flow computations, the shock Mach number is obtained by interpolation of

$$(X/D)^2 = 0.49\gamma [2 + (\gamma-1)M^2]^{\gamma/(\gamma-1)} [\gamma+1]^{-1/\gamma-1} \div [2\gamma M^2 - (\gamma-1)] \quad (4)$$

Presented as Paper 81-1109 at the AIAA 16th Thermophysics Conference, Palo Alto, Calif., June 23-25, 1981; received Dec. 21, 1982; revision received June 20, 1983.

*Supervisory Aerospace Engineer, Launch and Flight Division. Associate Fellow AIAA.

which permits determination of the flow properties behind the shock based upon the known muzzle exit conditions. Presuming a spherically symmetric core flow and using lateral Mach disk dimensions from experiment,[1] the mass flow through this shock is

$$\alpha = 0.96[X/D]^2 M[(\gamma+1)/(2+(\gamma-1)M^2)]^{(\gamma+1)/2(\gamma-1)} \quad (5)$$

Finally, Yousefian postulates that behind the Mach disk there is a spatially uniform jet at atmospheric pressure having properties determined by mass averaging the flow through the Mach disk and intercepting shocks, assumed to be weak, isentropic waves.

Yousefian provides the most realistic model of muzzle flash to date, but does not treat the influence of the basic unsteady nature of gun exhaust nor the effect of muzzle devices common to large caliber gun systems. In the current Note, these effects are examined using a methodology which simply combines the near muzzle flow description of Yousefian with the ignition analysis of Carfagno.

Analysis

The ignition in the exhaust plume of the 155 mm M109 self-propelled howitzer is considered. To reduce the recoil impulse, propellant gas flow is deflected rearward using a double baffle, muzzle brake. Examination of high-speed photographs shows that with the brake installed, emissions indicative of secondary combustion occur throughout the plume; however, when it is removed, luminosity is seen only very early in the emptying cycle and is soon extinguished. This behavior is examined by calculating mixture temperatures for each case.

The exhaust is assumed to be steady with muzzle conditions computed at the time of shot ejection. For the M203 charge, the exit Mach number is sonic and $u^* = 872$ m/s, $p^*/p_\infty = 630$, and $T^* = 1918$ K. The flow internal to the brake is taken as a series of shock-expansion processes. Impingement of the propellant gas jet on baffle surfaces, located 1.7 and 4.0 diameters from the muzzle, forms a normal shock followed by expansion to sonic conditions in the projectile passageway. The variations in temperature with mixture ratio for cases with and without the brake are compared in Fig. 2. With a bare muzzle, the temperature remains well below the ignition limit for all mixture ratios. When the muzzle brake is in place, ignition is predicted to occur. The increased mixture temperatures are directly associated with the presence of strong normal shocks in the brake flow. Another factor to be investigated is the influence of flow transience.

The gun exhaust is characterized by two levels of temporal variation: first, the growth of the plume is grossly unsteady

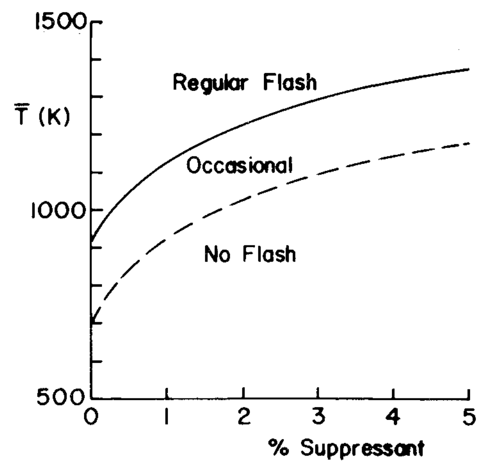

Fig. 1 Ignition temperature limits of Carfagno[2] as a function of amount of flash suppressant in propellant.

Table 1 Muzzle exit property variation for 155 mm firing at zone 8S

t, ms	u^*, m/s	p^*/p_∞	T^*, K
0	872	630	1918
10	734	123	1359
20	662	44	1107
30	594	15	890

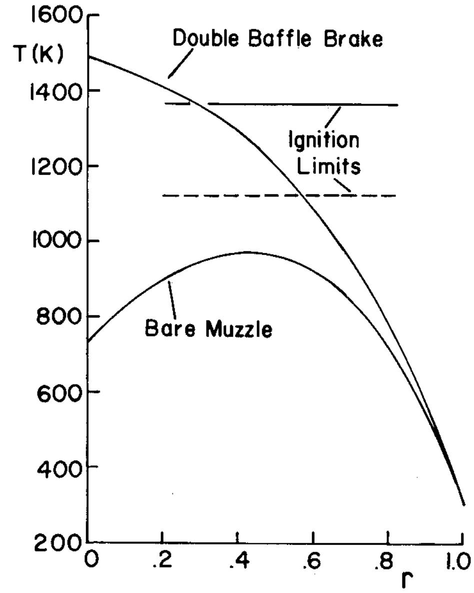

Fig. 2 Comparison of mixture temperatures for cases with and without muzzle brake mounted on 155-mm howitzer.

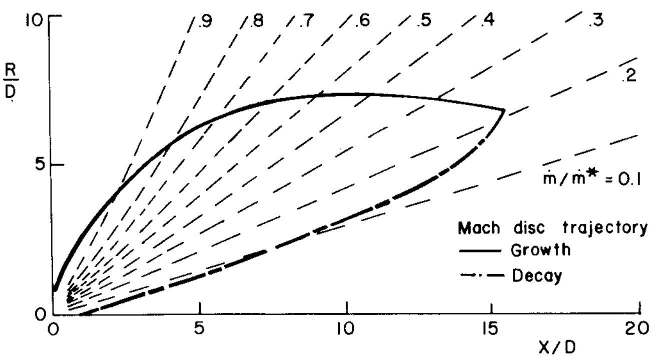

Fig. 3 Measured trajectory of triple point.

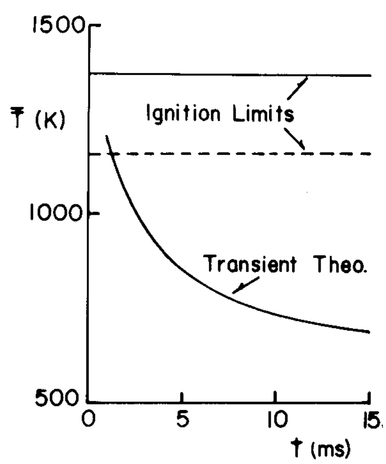

Fig. 4 Mixture temperature vs emptying time for 155-mm howitzer.

and, second, the muzzle properties change continuously as the weapon empties. While the present model cannot treat the actual flow, estimates are possible of the global influence of these effects. For the M109A1 howitzer, the decay in exit properties is given in Table 1.

The growth and decay of the inviscid core are approximated using a one-dimensional, time-dependent calculation[4] to describe the flow along the axis of symmetry coupled to experimental results[1] to define the off-axis shock structure. The data describe the trajectory of the triple point marking the junction of the intercepting shock and Mach disk, Fig. 3. Superimposed on this figure are computed contours of relative mass flux showing that during the initial growth of the plume nearly all of the exhaust mass is processed through the Mach disk; whereas, later in the emptying cycle, the influence of the Mach disk is greatly diminished.

Using the computed Mach disk velocity, a relative flow Mach number and shock jump conditions are evaluated. For each time considered, the mixture temperatures are determined. The maximum value of this parameter over the interval $0.2<r<0.8$ is shown in Fig. 4. At the beginning, the temperature is very high due to the large mass flow through the Mach disk. As the growth of the plume continues, the mixture temperatures monotonically decay and at later times are dominated by the muzzle exit properties and decreasing mass flow through the Mach disk. The calculation predicts highest probability of ignition early in the exhaust cycle; a conclusion supported in part by observations of actual firings showing ignition soon after shot ejection.

Summary and Conclusions

A simple model of ignition in gun exhaust plumes is presented. While it treats the gasdynamics and chemistry in an approximate fashion, the technique can be easily coupled to existing inviscid analyses of muzzle flow and used to point out qualitative variations in flash processes. Calculations clearly display the strong influence of muzzle devices and time dependence upon the ignition process.

References

[1]Schmidt, E. and Shear, D., "Optical Measurements of Muzzle Blast," *AIAA Journal*, Vol. 13, Aug. 1975, pp. 1086-1091.

[2]Carfagno, S., *Handbook on Gun Flash*, The Franklin Institute, Philadelphia, Pa., 1961.

[3]Yousefian, V., "Muzzle Flash Onset," Aerodyne Research, Inc., Bedford, Mass., ARI-RR-161.1, May 1979.

[4]Erdos, J. and DelGuidice, P., "Calculation of Muzzle Blast Flowfields," *AIAA Journal*, Vol. 13, Aug. 1975, pp. 1048-1055.

Adhesive Bonded Orthotropic Structures with a Part-Through Crack

C. S. Hong* and H. S. Ro†

Korea Advanced Institute of Science and Technology, Seoul, Korea

Introduction

IN recent years, considerable attention has been paid to the problem of adhesive bonded joints, as a result of growing interest in the damage-tolerant design of aircraft structures. Composite materials, due to their high strength-to-weight ratio, are being widely used in aircraft structures with adhesive bonded joints. Structural reliability is one of the main concerns of analytical and experimental research.

Several studies have been made on the problem of adhesively bonded structures.[1-6] Keer et al.[1] solved the problem of a cracked plate by using Fourier transform techniques and reduced it to a solution by integral equation. Arin and Erdogan[2-4] used a complex variable formulation to equations. Ko[5] analyzed an orthotropic sandwich plate containing a part-through crack subjected to in-plane mixed mode tractions. He formulated the problem and reduced it to a set of integral equations, but did not obtain the numerical solution of the equations. Ratwani[6] outlined finite element and mathematical methods of analysis for a two-isotropic-ply, adhesively bonded structure. The purpose of this Note is to extend Ratwani's isotropic structure solution to adhesive bonded orthotropic structures with a part-through crack. Some numerical results for stress intensity factors are presented for various values of crack length and adhesive thickness.

Formulation of the Problem

The orthotropic plate with a crack and a sound orthotropic plate are of the same width, and are assumed infintely wide. Consider the adhesively bonded structure of Fig. 1a, consisting of two plates with thickness h_1 and h_2, respectively, and bonded through an adhesive layer of constant thickness h_a. The plate is subjected to forces T_x and T_y per unit length of the plate. Plate 1 is assumed to have a through-crack and a debond in the adhesive around the crack.

In Fig. 1a, the size of the debond is shown to be the same as the length of the crack. If the initial debonding size in the adhesive is large, it is possible that the crack length will be shorter than the debond. However, this problem can still be formulated in a similar manner. The analysis of the adhesively bonded structure in Fig. 1a will be based on the following assumptions. The plate and the adhesive layer are homogeneous and linearly elastic. The thickness of the adhesive is small compared to the thickness of the adherends;

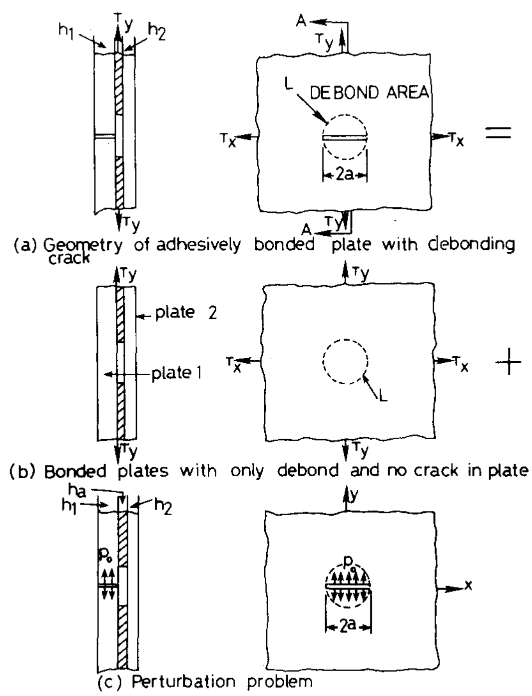

Fig. 1 Superposition technique for an adhesively bonded plate with a debonding area.

Received April 24, 1981; revision received Jan. 19, 1983.

*Associate Professor, Dept. of Aeronautical Engineering. Member AIAA.

†Graduate Student, Dept. of Mechanical Engineering; presently with Samsung Heavy Industries Co., Ltd., Changwon, Korea.